

## Phase diagram of a quantum Hall pseudospin ferromagnet in a two-subband electron system

This article has been downloaded from IOPscience. Please scroll down to see the full text article.

2009 J. Phys.: Condens. Matter 21 455802

(<http://iopscience.iop.org/0953-8984/21/45/455802>)

View [the table of contents for this issue](#), or go to the [journal homepage](#) for more

Download details:

IP Address: 129.252.86.83

The article was downloaded on 30/05/2010 at 06:01

Please note that [terms and conditions apply](#).

# Phase diagram of a quantum Hall pseudospin ferromagnet in a two-subband electron system

Xiao-Jie Hao<sup>1</sup>, Tao Tu<sup>1</sup>, Gang Cao<sup>1</sup>, Guang-Can Guo<sup>1</sup>,  
Hong-Wen Jiang<sup>2</sup> and Guo-Ping Guo<sup>1</sup>

<sup>1</sup> Key Laboratory of Quantum Information, University of Science and Technology of China, Chinese Academy of Sciences, Hefei 230026, People's Republic of China

<sup>2</sup> Department of Physics and Astronomy, University of California at Los Angeles, 405 Hilgard Avenue, Los Angeles, CA 90095, USA

E-mail: [tutao@ustc.edu.cn](mailto:tutao@ustc.edu.cn) and [jiangh@physics.ucla.edu](mailto:jiangh@physics.ucla.edu)

Received 10 July 2009, in final form 15 September 2009

Published 23 October 2009

Online at [stacks.iop.org/JPhysCM/21/455802](http://stacks.iop.org/JPhysCM/21/455802)

## Abstract

We employ the self-consistent local density approximation and the microscopic Hartree–Fock theory to investigate the quantum Hall pseudospin ferromagnets at the Landau levels degenerate regime of a single quantum well with two-subbands filled. We carry out a detailed calculation of the pseudospin anisotropy energy using real experimental parameters and obtain the phase diagrams that would be accessed experimentally by changing the electron density and the bias voltage. We find that an easy-plane and easy-axis quantum Hall pseudospin ferromagnet can form at total filling factors  $\nu = 3$  and  $\nu = 4$ , respectively, which are consistent with experimental observation. Our study provides some insight into the symmetry of the ground state and may help in understanding the underlying mechanism.

(Some figures in this article are in colour only in the electronic version)

## 1. Introduction

The two-dimensional electron gas in a strong magnetic field with multi-fold degeneracy has attracted considerable and continuous interest in recent years [1]. Besides the anisotropic phases at half-filling factor reported in recent years, for instance, stripes [2, 3], anisotropic Fermi liquids [4], liquid crystalline phases [5, 6], etc, there is another class of broken symmetry states with pseudospin anisotropy in the multi-component quantum Hall system. In a multi-component quantum Hall system, the electron states are labeled as Landau levels (LLs) with different layer [7], subband [8–10], valley [11], orbital and spin indices. When multiple LLs are tuned to degeneracy either by charge density or magnetic field, electron–electron interactions become prominent and lead to fruitful competing orders and broken symmetry states. Among these systems, a single quantum well with two-subbands occupied [8–10] is an ideal laboratory to investigate the above interesting issues. Recent transport measurement has shown evidence of the formation of quantum Hall ferromagnets of pseudospins, where the pseudospin represents the subband

degree of freedom. The quantum Hall pseudospin ferromagnet (QHPFs) can either be easy-axis or easy-plane anisotropy, depending on the details of LL crossing configurations [8, 9]. Although a number of interesting phenomena have been exploited experimentally in this system [9, 10, 12–15], systematic theoretical work is lacking.

In this paper we give the theoretical framework of the two-subband quantum Hall system and calculate the pseudospin anisotropy energy using real sample parameters in experiments [9, 12, 13]. The results show the ground states at total filling factor  $\nu = 3$  and 4 are expected to be easy-plane and easy-axis QHPFs, respectively, which are consistent with the experimental observation. As we will discuss in this paper, the gate bias voltage, which affects the spatial distributions of the wavefunctions of the two subbands, plays an important role in the formation of easy-plane or easy-axis QHPFs.

## 2. Hartree–Fock theory of two-subband system

The pseudospin ferromagnet has been best illustrated in the bilayer quantum Hall system at total filling factor  $\nu = 1$ ,

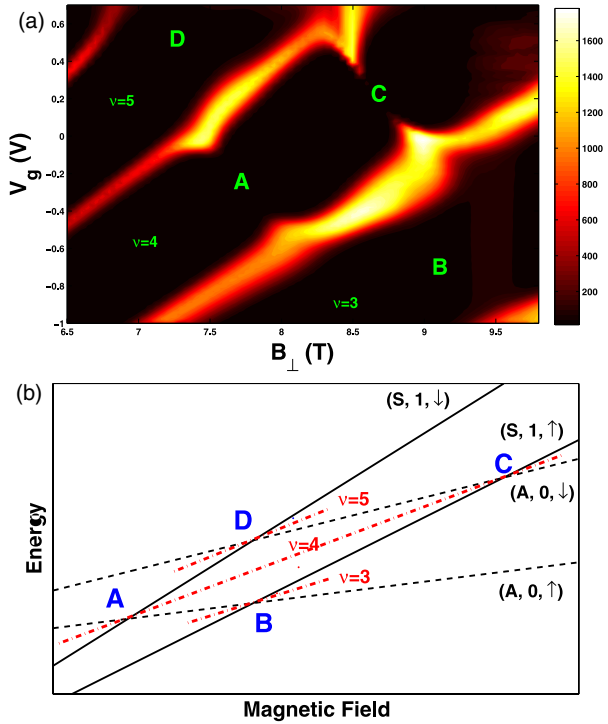


**Figure 1.** (a) The experimental measured longitudinal resistance  $R_{xx}$  in the gate voltage ( $V_g$ )—perpendicular magnetic field ( $B_{\perp}$ ) diagram at filling factor  $\nu = 3, 4, 5$  of a 24 nm wide GaAs/AlGaAs quantum well [9, 12, 13]. (b) Schematic drawing of the crossing levels between different subband, orbital and spin indices Landau levels at four corresponding points marked by A, B, C, D in (a). The red dot-dash lines indicate the Fermi levels at filling factors  $\nu = 3, 4, 5$ .

where the pseudospin represents the layer degree of freedom [16–19]. Here we apply the pseudospin language to describe a two-subband two-dimensional electron system, in which the LLs are labeled as  $|(\xi, n, s)\rangle$ , where  $\xi = S/A$  is the first/second subband (in the non-biased quantum well, also called symmetry/antisymmetry subband) index,  $n = 0, 1, \dots$  is Landau level in-plane orbit radius quantum number, and  $s = \uparrow, \downarrow$  represents real spin. When two LLs are brought close to degeneracy but still sufficiently far from other LLs, one of them can be regarded as pseudospin up ( $\sigma = \uparrow$ ) and the other as pseudospin down ( $\sigma = \downarrow$ ).

In a series of experimental work [9, 12, 13], the observed square structure demonstrates the opening gaps of the easy-plane or easy-axis pseudospin ferromagnetic states, respectively at the level crossing points of B, D and A, C, as depicted in figure 1(a). Here point A corresponds to the degeneracy point of  $|(S, 1, \downarrow)\rangle$  and  $|(A, 0, \uparrow)\rangle$ , point B corresponds to that of  $|(S, 1, \uparrow)\rangle$  and  $|(A, 0, \uparrow)\rangle$ , point C corresponds to that of  $|(S, 1, \uparrow)\rangle$  and  $|(A, 0, \downarrow)\rangle$ , and point D corresponds to that of  $|(S, 1, \downarrow)\rangle$  and  $|(A, 0, \downarrow)\rangle$ , as illustrated schematically in the Landau level fan diagram figure 1(b). Then we can denote  $|(S, 1, \uparrow)\rangle$  as pseudospin up ( $\sigma = \uparrow$ ) and  $|(A, 0, \uparrow)\rangle$  as pseudospin down ( $\sigma = \downarrow$ ) at filling factor  $\nu = 3$ . At filling factor  $\nu = 4$ , we denote  $|(S, 1, \downarrow)\rangle$  or  $|(S, 1, \uparrow)\rangle$  as pseudospin up ( $\sigma = \uparrow$ ) and  $|(A, 0, \uparrow)\rangle$  or  $|(A, 0, \downarrow)\rangle$  as pseudospin down ( $\sigma = \downarrow$ ).

The many-body Hamiltonian for crossing Landau level electrons in two-subband system has the following form:

$$H = \sum_{\sigma_1, \sigma_2, k} c_{\sigma_1 k}^{\dagger} h_{\sigma_1 \sigma_2}^0 c_{\sigma_2 k} + \frac{1}{2} \sum_{\substack{\sigma_1, \sigma_2, \sigma'_1, \sigma'_2 \\ k_1, k_2, k'_1, k'_2}} c_{\sigma_1 k_1}^{\dagger} c_{\sigma_2 k_2}^{\dagger} c_{\sigma'_2 k'_2} c_{\sigma'_1 k'_1} \times \langle \sigma_1 k_1, \sigma_2 k_2 | V | \sigma'_1 k'_1, \sigma'_2 k'_2 \rangle, \quad (1)$$

where  $c_{\sigma, k}^{\dagger}$  creates the single-particle state  $\psi_{\sigma, k}(\vec{r})$  which contains the growth direction subband wavefunction  $\lambda_{\xi}(z)$  and the in-plane LL wavefunction  $L_{n, s, k}(x, y)$ :

$$\psi_{\sigma, k}(\vec{r}) = \lambda_{\xi}(z) L_{n, s, k}(x, y), \quad (2)$$

$k$  is the wavevector label,  $h^0$  is the single-particle energy including the external bias potential, tunneling gap, cyclotron, and Zeeman energies, and  $V$  is the 2D Coulomb interaction. While pseudospin up and pseudospin down LLs are degenerate, but the number of electrons is not enough to fill all the two LLs, electrons will stay in a broken symmetry ground state. Actually, the state electrons choose a linear combination of two pseudospin LLs which minimizes the system total energy. Typically, the many-body ground state can be written as follows:

$$|\Psi[\hat{m}]\rangle = \prod_{k=1}^{N_{\phi}} c_{\hat{m}, k}^{\dagger} |0\rangle, \quad (3)$$

where  $c_{\hat{m}, k}^{\dagger}$  creates the single-particle state oriented in a certain unit vector  $\hat{m} = (\sin \theta \cos \varphi, \sin \theta \sin \varphi, \cos \theta)$  with wavefunction:

$$\psi_{\hat{m}, k}(\vec{r}) = \cos\left(\frac{\theta}{2}\right) \psi_{\uparrow, k}(\vec{r}) + \sin\left(\frac{\theta}{2}\right) e^{i\varphi} \psi_{\downarrow, k}(\vec{r}). \quad (4)$$

Before further calculation, there are some issues that may need to be clarified. Firstly, there is some essential similarity between the two-subband system and bilayer system (double quantum well) [18, 19] from the viewpoint of pseudospin theory. That is why all the pseudospin language theory used in bilayer systems [18] can be applied directly to the two-subband system as shown in this paper. Secondly, since the wavefunction of the first and second subband are spatially located in the same well, direct spatial coupling between the two sets of Landau levels can potentially give rise to a correlation different from the spatially separated cases. Also the barrier in a single quantum well is soft, originating from Coulomb repulsion. As a result of this softness, the tunneling gap can not be treated as an one-body field acting on the pseudospin levels but will depend on the pseudospin orientation in the ground state [20]. Thus in the present work we have to use the self-consistent local density approximation (LDA) for the calculation of the growth direction subband wavefunction to account for mixing of higher electrical subbands in any sample geometry. Thirdly, in a similar study [21] the pseudospin (representing the LL index degree of freedom) anisotropy is driven by the coincidence of two different Landau levels at large magnetic field tilting angles, which is not possibly consistent with our study in zero in-plane magnetic field.

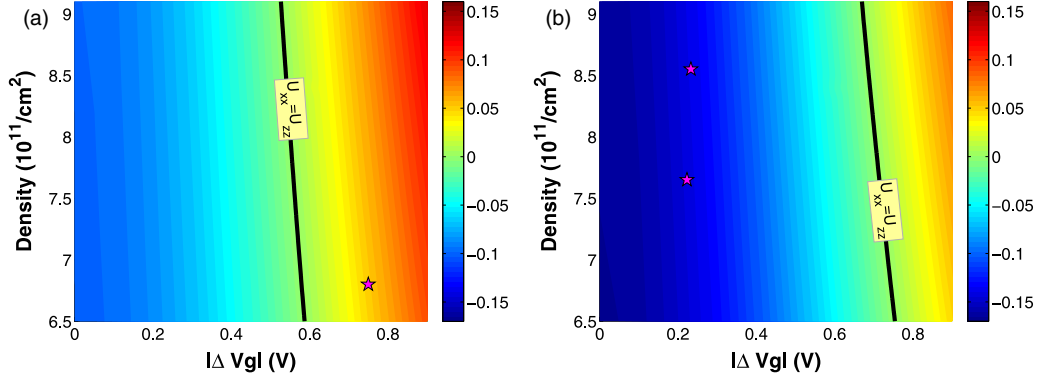


**Figure 2.** Phase diagram of  $U_{zz} - U_{xx}$  (unit:  $e^2/\epsilon l_0$ ) at filling factor (a)  $\nu = 3$  and (b)  $\nu = 4$ . In the  $U_{zz} - U_{xx} < 0$  (left/blue) region the easy-axis QHPF is energetically favorable while in the  $U_{zz} - U_{xx} > 0$  (right/red) region, the easy-plane QHPF is favorable. Black lines in each figure labeled by  $U_{xx} = U_{zz}$  show the critical positions where a quantum phase transition from easy-axis to easy-plane QHPF occurs. The three stars in these two figures correspond to the  $\nu = 3$  and 4 crossing points measured in the experiments (see points B, A, C in figure 1) [9, 12].

Then the Hartree–Fock energy of the system can be obtained as the following:

$$\begin{aligned}
 E_{\text{HF}}(\hat{m}) &\equiv \frac{\langle \Psi[\hat{m}] | H | \Psi[\hat{m}] \rangle}{N_\phi} \\
 &= - \sum_{i=x,y,z} \left( E_i - \frac{1}{2} U_{1,i} - \frac{1}{2} U_{i,1} \right) m_i \\
 &\quad + \frac{1}{2} \sum_{i,j=x,y,z} U_{i,j} m_i m_j. \quad (5)
 \end{aligned}$$

Whether the ground state is easy-axis or easy-plane only depends on the quadratic coefficient in the pseudospin magnetization  $m_i$  (i.e. the pseudospin anisotropy energy  $U_{xx}$ ,  $U_{yy}$  and  $U_{zz}$ ):

$$U_{ij} = \frac{1}{4} \int \frac{d^2 \vec{q}}{(2\pi)^2} v_{ij}(0) - \frac{1}{4} \int \frac{d^2 \vec{q}}{(2\pi)^2} v_{ij}(\vec{q}). \quad (6)$$

The first  $\vec{q} = 0$  term in equation (6) is the Hartree term and the second term is the Fock term.  $v_{ij}(\vec{q})$  can be expanded to the sum of several pseudospin matrix elements  $v_{\sigma'_1, \sigma'_2, \sigma_1, \sigma_2}(\vec{q})$ , which are products of the subband and the in-plane parts. If  $U_{zz} < U_{xx} = U_{yy}$ , the system is in easy-axis QHPF, which means the pseudospin magnetization  $\hat{m}$  is aligned either up or down; and if  $U_{zz} > U_{xx} = U_{yy}$ , the system is in easy-plane QHPF, which is a coherent superposition of the two pseudospin LLs.

### 3. Calculation of the growth direction subband wavefunction

Since the in-plane LL wavefunction can be obtained analytically, we numerically calculate the growth direction ( $z$  direction) subband wavefunction  $\lambda_\xi(z)$  in equation (2) using self-consistent LDA [22] at zero in-plane magnetic field. In the self-consistent LDA method, wavefunction  $\lambda(z)$  is given by the Schrödinger equation:

$$\left( -\frac{1}{2m^*} \frac{\partial^2}{\partial z^2} + V_b(z) + V_{\text{gate}}(z) + V_{\text{xc}}(z) + V_{\text{H}}(z) \right) \lambda_i(z) = \epsilon_i \lambda_i(z). \quad (7)$$

Here  $m^*$  is the effective electron mass in GaAs,  $V_b$  corresponds to the conduction band discontinuity,  $V_{\text{gate}}$  is the bias potential caused by the difference of front and back gate voltages  $|\Delta V_g|$ ,  $V_{\text{xc}}$  refers to the exchange–correlation potential related to the electron charge distribution  $n(z)$  (we use the form of  $V_{\text{xc}}$  given by Hedin and Lundqvist [23]). The Hartree term  $V_{\text{H}}$  due to electrostatic potential is given in the Poisson equation:

$$V_{\text{H}}(z) = -\frac{2\pi e^2}{\epsilon} \int dz' |z - z'| n(z'). \quad (8)$$

The subband energies  $\epsilon_\xi$ , wavefunctions  $\lambda_\xi(z)$  and the electron charge distributions  $n_\xi(z)$  of both subbands can be calculated by solving the Schrödinger equation (7) and the Poisson equation (8) simultaneously [24].

### 4. Phase diagram of quantum Hall pseudospin ferromagnet

Taking the unit of energy as  $e^2/\epsilon l_B$  ( $l_B$  is the magnetic length), we calculate the pseudospin anisotropy energy  $U_{xx}$ ,  $U_{yy}$  and  $U_{zz}$  at filling factor  $\nu = 3$  and 4. The experimental parameters we use are from a single wide (24 nm) GaAs/AlGaAs quantum well, with a global top gate approximately 350 nm away from the center of the quantum well. The total density of the sample, which is proportional to the gate voltage in a certain range, is about  $8.0 \times 10^{-11} \text{ cm}^{-2}$  at bias gate voltage  $\Delta V_g = 0 \text{ V}$  [9, 12, 13]. At total filling factor  $\nu = 3$ ,  $U_{xx} \equiv U_{yy} = -0.370 < U_{zz} = 0.017$ , so the system will stay in an easy-plane QHPF. At one degenerate point of total filling factor  $\nu = 4$ ,  $U_{xx} \equiv U_{yy} = 0 > U_{zz} = -0.1266$ , and at the other degenerate point  $U_{xx} \equiv U_{yy} = 0 > U_{zz} = -0.1293$ . The two energy differences of  $U_{zz} - U_{xx}$  at  $\nu = 4$  indicate the easy-axis QHPF ground states.

To illustrate the evolution from easy-axis QHPF to easy-plane QHPF, we calculate the phase diagrams of  $U_{zz} - U_{xx}$  as a function of bias gate voltage  $|\Delta V_g|$  and total density  $n$  at filling factor  $\nu = 3$  (figure 2(a)) and  $\nu = 4$  (figure 2(b)). In the following, for consistency, we choose  $e^2/\epsilon l_0$  ( $l_0 = 10 \text{ nm}$ ) as the unit of energy. In the left/blue (right/red) parts of

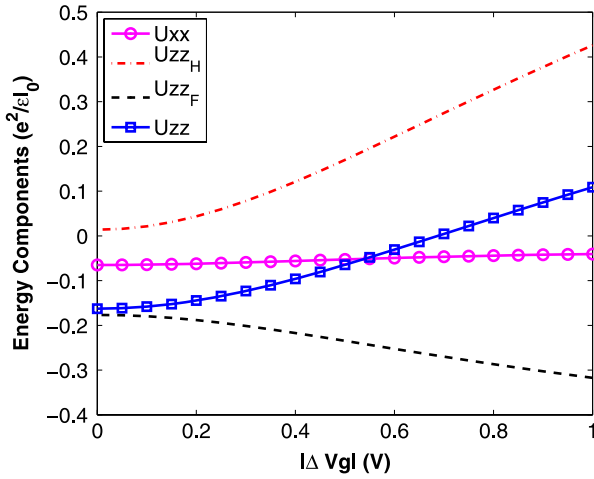


**Figure 3.** Components of anisotropy energy  $U_{xx}$  and  $U_{zz}$  versus bias voltage  $|\Delta V_g|$ . Except for  $U_{xx} \equiv 0$  at  $\nu = 4$ , all the other terms are the same at filling factor  $\nu = 3$  and 4.  $U_{zzH}$  and  $U_{zzF}$  correspond to the Hartree term and Fock term in the calculation of  $U_{zz}$ .

each figure (figures 2(a) and (b)), where  $U_{zz} < (>)U_{xx}$ , the easy-axis (easy-plane) has the lower electron interaction energy. Along the black line at the phase boundary labeled as  $U_{xx} = U_{zz}$ , the QHPF is isotropic. From figure 2, we find that the anisotropy energy difference  $U_{zz} - U_{xx}$  is very sensitive to the bias voltage  $|\Delta V_g|$ . If we could vary the gate voltage across the isotropic line  $U_{xx} = U_{zz}$  from left to right in a determined density, a quantum phase transition from easy-axis to easy-plane QHPF would happen.

In order to make a comparison of the effect of each term in anisotropy energy equation (6), we plot them as a function of  $|\Delta V_g|$  at a certain density of  $8.5 \times 10^{11} \text{ cm}^{-2}$  in figure 3. Note that the dominant term in  $U_{zz} - U_{xx}$  is the Hartree term  $U_{zzH}$ , which is due to the electrostatic potential of electrons. It shows that the  $U_{zzH}$  term increases immediately with the increasing bias voltage  $|\Delta V_g|$ .

To examine what the role the bias voltage plays in the determination of the easy-plane or easy-axis QHPF, we give some results of  $z$  direction subband wavefunctions in the figure 4. We define an effective subband separation  $\Delta d = |d_S - d_A|$  to describe the distance between the cores of the first and second subband wavefunctions. The core of a subband wavefunction is defined as

$$d_{S(A)} = \int |\lambda_{S(A)}(z)|^2 z dz. \quad (9)$$

The  $|\Delta d|$  as a function of bias voltage is plotted in figure 4, with some demonstrations of quantum well configurations and subband wavefunctions in different bias voltages ( $|\Delta V_g| = 0.0, 0.3, \text{ and } 1.0 \text{ V}$ ), as well. The parameters in figure 4 are all selected from the same density  $8.5 \times 10^{11} \text{ cm}^{-2}$  in figure 3. It is obvious that the bias gate voltage changes the effective separation of two subbands while changing the well potential  $V_{\text{gate}}(z)$  in equation (7). The larger the bias voltage added, the farther the lowest two subbands are separated. Since at a well separated  $z$  direction wavefunction configuration, all the electrons near the Fermi level filling the same subband, i.e. the

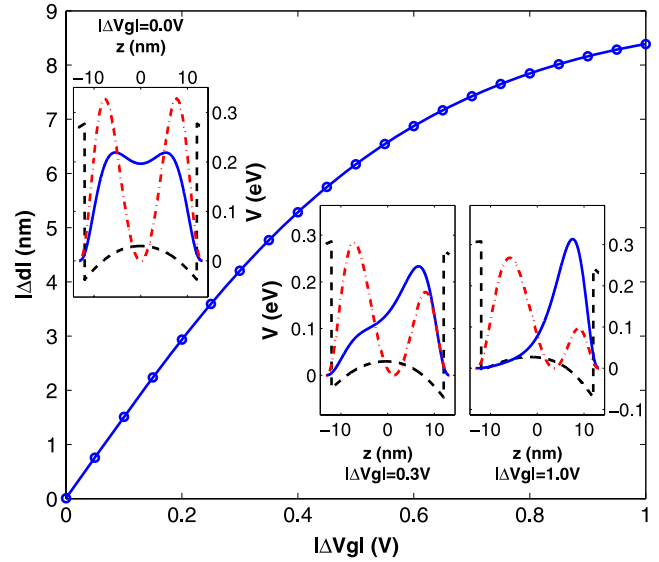


**Figure 4.** Effective subband separation  $|\Delta d|$  as a function of bias gate voltage  $|\Delta V_g|$  at the density of  $8.5 \times 10^{11} \text{ cm}^{-2}$ . Three insets show the well profiles (black dashed lines) with the first (blue solid lines) and second (red dash-dot lines) subband wavefunctions at different bias voltage:  $|\Delta V_g| = 0.0, 0.3, \text{ and } 1.0 \text{ V}$ .

same pseudospin level, will raise a larger electrostatic energy, the easy-axis QHPF is not favorable. Thus an easy-plane QHPF can save more Hartree energy in the larger bias voltage situation (filling factor  $\nu = 3$  in the experiment). On the other hand, when the potential of the quantum well maintains a good symmetry in the small bias voltage limit (filling factor  $\nu = 4$  in the experiment), electrons can pick up one of the two pseudospin levels, i.e. forming the easy-axis QHPF to keep the Hartree energy minimal and avoid the energetic penalty from inter-subband tunneling as well. From this point of view, if the quantum well becomes narrower, the easy-axis anisotropy is more likely to happen due to closer a distance between two-subband wavefunctions. This conclusion is also consistent with the figure 5 in [18]. In their bilayer system, the easy-axis state is more likely to form in a smaller layer separation [18]. Here we can see how important the growth direction wavefunction is in affecting the pseudospin orientation.

Besides the leading contribution from the Hartree term  $U_{zzH}$  mentioned above, there is also a minor Fock term playing a role. The anisotropy energy  $U_{xx}$  or  $U_{yy}$  is constituted of a Hartree part and a Fock part (see equation (6)). In our numerical calculation, we find that the Hartree terms of  $U_{xx}$  and  $U_{yy}$  are always zero at both  $\nu = 3$  and 4. The only non-zero term in  $U_{xx}$  or  $U_{yy}$  is the Fock term  $U_{xxF} \equiv U_{yyF} < 0$  at filling factor  $\nu = 3$ , which is due to the exchange interaction. It implies that at filling factor  $\nu = 4$ , where pseudospin up  $\sigma = \uparrow (|(S, 1, \downarrow)\rangle \text{ or } |(S, 1, \uparrow)\rangle)$  and pseudospin down  $\sigma = \downarrow (|(A, 0, \uparrow)\rangle \text{ or } |(A, 0, \downarrow)\rangle)$  have opposite real spins, the easy-plane anisotropy, in which the electrons stay in both subband equally, would cost much more exchange energy. But at  $\nu = 3$  the pseudospin up  $\sigma = \uparrow (|(S, 1, \uparrow)\rangle)$  and pseudospin down  $\sigma = \downarrow (|(A, 0, \uparrow)\rangle)$  have the same spin. Then there is no such problem need to be considered. Therefore, the easy-axis QHPF is more likely to happen at total filling factor  $\nu = 4$  than  $\nu = 3$ .



In summary, the bias gate voltage added to the sample changes the quantum well profile in the growth direction as well as the spatial separation of the lowest two subband wavefunctions. For a larger bias gate voltage, the potential of the well is much more skewed, so the two subband wavefunctions locate on the opposite sides of the quantum well (inset of figure 4). As a result, the Hartree energy will arise if all the electrons stay in one narrow subband or pseudospin level. Thus an easy-plane QHPF, in which the electrons fill the two pseudospin levels equally, is more energetically favorable at a large bias gate voltage (filling factor  $\nu = 3$  in the experiment). In addition, a state with opposite real spins will expend more exchange energy, so the easy-plane QHPF is more easily formed at a pseudospin configuration in which the two pseudospin level have the same real spin (filling factor  $\nu = 3$  in the experiment).

## 5. Conclusion

We explain the recent observation of transport measurements in a two-subband system in terms of the unique physics of a quantum Hall pseudospin ferromagnet. Applying a microscopic Hartree–Fock theory, we show that the anisotropy properties of the ground state are determined by a competition of the electrostatic and exchange energies, unlike the novel anisotropic states at half-filling factor [2–6]. The mean field pseudospin theory used in this paper is able to account quantitatively for basic characteristics of possible broken symmetry states in a two-subband system. Close to the quantum phase transition region (see the black line in figure 2), fluctuations will be important [25], and including quantum fluctuations [26] may help with a more complete understanding. Furthermore, going beyond the Hartree–Fock approximations used in this paper one may be able to stabilize other many-body phases with broken symmetries, most notably the skyrmion stripe phase [19]. These important topics will be discussed elsewhere.

## Acknowledgments

This work at USTC was funded by the National Basic Research Program of China (Grants Nos 2006CB921900 and 2009CB929600), the Innovation funds from the Chinese Academy of Sciences, and the National Natural Science Foundation of China (Grants Nos 10604052, 10874163

and 10804104). The work at UCLA was supported by the NSF under Grant No. DMR-0804794.

## References

- [1] For a review, see experimental chapter by J P Eisenstein and theoretical chapter by S M Girvin and A H MacDonald, Das Sarma S and Pinczuk A (ed) 1997 *Perspectives on Quantum Hall Effects* (New York: Wiley)
- [2] Lilly M P, Cooper K B, Eisenstein J P, Pfeiffer L N and West K W 1999 *Phys. Rev. Lett.* **82** 394
- [3] Fogler M M 2002 *Int. J. Mod. Phys. B* **16** 2924
- [4] Doan Q M and Manousakis E 2008 *Phys. Rev. B* **78** 075314
- [5] Ciftja O and Wexler C 2008 *Physica B* **403** 1511
- [6] Ciftja O and Wexler C 2002 *Phys. Rev. B* **65** 205307
- [7] Murphy S Q, Eisenstein J P, Boebinger G S, Pfeiffer L N and West K W 1994 *Phys. Rev. Lett.* **72** 728
- [8] Muraki K, Saku T and Hirayama Y 2001 *Phys. Rev. Lett.* **87** 196801
- [9] Zhang X C, Martin I and Jiang H W 2006 *Phys. Rev. B* **74** 073301
- [10] Ellenberger C, Simovic B, Leturcq R, Ihn T, Ulloa S E, Ensslin K, Driscoll D C and Gossard A C 2006 *Phys. Rev. B* **74** 195313
- [11] Vakili K, Gokmen T, Gunawan O, Shkolnikov Y P, De Poortere E P and Shayegan M 2006 *Phys. Rev. Lett.* **97** 116803
- [12] Guo G P, Zhao Y J, Tu T, Hao X J, Zhang X C, Guo G C and Jiang H W 2008 *Phys. Rev. B* **78** 233305
- [13] Guo G P, Zhao Y J, Tu T, Hao X J, Guo G C and Jiang H W 2009 arXiv:0904.0917
- [14] Duarte C A, Gusev G M, Quivy A A, Lamas T E, Bakarov A K and Portal J C 2007 *Phys. Rev. B* **76** 075346
- [15] Yu G, Lockwood D J, SpringThorpe A J and Austing D G 2007 *Phys. Rev. B* **76** 085331
- [16] MacDonald A H, Platzman P M and Boebinger G S 1990 *Phys. Rev. Lett.* **65** 775
- [17] Yang K, Moon K, Zheng L, MacDonald A H, Girvin S M, Yoshioka D and Zhang S C 1994 *Phys. Rev. Lett.* **72** 732
- [18] Jungwirth T and MacDonald A H 2000 *Phys. Rev. B* **63** 035305
- [19] Wang D W, Demler E and Das Sarma S 2003 *Phys. Rev. B* **68** 165303
- [20] Piazza V, Pellegrini V, Beltram F, Wegscheider W, Jungwirth T and MacDonald A H 1999 *Nature* **402** 638
- [21] Jungwirth T, Shukla S P, Smrčka L, Shayegan M and MacDonald A H 1998 *Phys. Rev. Lett.* **81** 2328
- [22] Stern F and Das Sarma S 1984 *Phys. Rev. B* **30** 840
- [23] Hedin L and Lundqvist B I 1971 *J. Phys. C: Solid State Phys.* **4** 2064
- [24] Blatt J M 1967 *J. Comput. Phys.* **1** 382
- [25] Yang K, Moon K, Belkhir L, Mori H, Girvin S M, MacDonald A H, Zheng L and Yoshioka D 1996 *Phys. Rev. B* **54** 11644
- [26] Moon K 1997 *Phys. Rev. Lett.* **78** 3741